

Zinc oxide nanoparticles induce toxicity in CAL 27 oral cancer cell lines by activating PINK1/Parkin-mediated mitophagy

Jianfeng Wang¹
Shutao Gao²
Shuyu Wang³
Zhaonan Xu³
Limin Wei³

¹Department of Orthodontics, School and Hospital of Stomatology, Wenzhou Medical University, Wenzhou, China; ²Department of Nuclear Medicine, Handan Central Hospital, Handan, China; ³Department of Pediatric Dentistry, School and Hospital of Stomatology, Wenzhou Medical University, Wenzhou, China

Background: Tongue squamous cell carcinoma (tongue cancer) is one of the most common malignancies in the oral maxillofacial region. The tumor easily relapses after surgery, and the prognosis remains poor. Recently, zinc oxide nanoparticles (ZnO NPs) were shown to target multiple cancer cell types. In this study, we aimed to elucidate the anticancer effect of ZnO NPs on CAL 27 human tongue cancer cells and identify the role of PINK1/Parkin-mediated mitophagy in this effect.

Materials and methods: We analyzed the dose-dependent cytotoxic effects of ZnO NPs on CAL 27 cells. Cells were cultured in media containing 0, 5, 10, 20, 30, 40, 50, 60, 70, 80, 90, or 100 µg/mL ZnO NPs for 24 h. We further examined the intracellular reactive oxygen species levels, monodansylcadaverine intensity and mitochondrial membrane potential following the administration of 25 µg/mL ZnO NPs for 4, 8, 12, or 24 h and investigated the role of PINK1/Parkin-mediated mitophagy in ZnO NP-induced toxicity in CAL 27 cells.

Results: The viability of CAL 27 cells decreased after treatment with increasing ZnO NP concentrations. The inhibitory concentration 50% of the ZnO NPs was calculated as 25 µg/mL. The ZnO NPs increased the intracellular reactive oxygen species levels and decreased the mitochondrial membrane potential in a time-dependent manner as well as activated the PINK1/Parkin-mediated mitophagy process in CAL 27 cells.

Conclusion: Based on our findings, ZnO NPs may possess potential anticancer activity toward tongue cancer cells.

Keywords: zinc oxide nanoparticles, mitophagy, tongue cancer, anticancer therapy

Introduction

Tongue squamous cell carcinoma (tongue cancer) is one of the most common malignancies of the oral maxillofacial region, and is characterized by high degree of local infiltration and a high rate of metastasis to the cervical lymph nodes.^{1,2} Currently, surgery, radiotherapy, and chemotherapy are the main treatments for tongue cancer; however, because the tumor easily relapses after surgery, the prognosis remains poor.³ With the recent improvements in nanomedicine, nanoparticles are now being perceived as promising cancer therapies.⁴⁻⁶ Zinc oxide nanoparticles (ZnO NPs) are metal nanoparticles that are widely used in many dental materials and cosmetic products.⁷⁻⁹ Recently, ZnO NPs were shown to target multiple cancer cell types, such as human hepatocellular carcinoma (HEPG2), human prostate cancer (PC3), non-small cell lung cancer (A549),¹⁰ human head and neck squamous cell carcinoma (HNSCC),¹¹ human colorectal adenocarcinoma cells, and human lymphoblastoid cells.¹² ZnO NPs exert their anticancer effects by inhibiting the proliferation of cancer cells, increasing the sensitivity of drug-resistant tumor

Correspondence: Limin Wei
School and Hospital of Stomatology,
Wenzhou Medical University,
Wenzhou 325027, China
Tel +86 I 373 834 0921
Email lwei525@wmu.edu.cn

cells, preventing the recurrence and metastasis of tumors, and restoring cancer immunosurveillance.¹³

Mitophagy is a critical process that maintains a healthy and functional mitochondrial network that responds to physiological adaptations and stress conditions during development, as well as throughout life.¹⁴ Based on accumulating evidence, it has been established that imbalanced mitophagy plays a dual role in the neoplastic progression and drug resistance of different tumor types.^{15,16} Both the inhibition and induction of mitophagy have been reported to enhance the drug sensitivity of different tumor cells.¹⁷ ZnO NPs significantly induce autophagy in human ovarian cancer cells by inducing reactive oxygen species (ROS) production.¹⁸ ZnO NPs with an average size of 50 nm may exert toxic effects on A549 cells by impairing autophagic flux, leading to cell death.¹⁹

However, the anticancer effect and mechanism of ZnO NPs on the CAL 27 human tongue cancer cell line have not been thoroughly investigated to date. The purpose of this study was to determine whether ZnO NPs exert an anticancer effect on CAL 27 human tongue cancer cells. Furthermore, the role of PINK1/Parkin-mediated mitophagy in ZnO NP-induced CAL 27 cytotoxicity was also investigated.

Materials and methods

Chemicals and reagents

ZnO NPs (average particle size: 50 nm), the autophagic vacuole indicator monodansylcadaverine (MDC), the intracellular ROS probe 2',7'-dichlorofluorescein diacetate (DCFH-DA), and the JC-1 mitochondrial membrane potential (MMP) Kit were obtained from Sigma-Aldrich Chemical Co (Sigma-Aldrich Co., St Louis, MO, USA). The CAL 27 human tongue cancer cell line was purchased from Cell Bank of the Chinese Academy of Sciences (Shanghai, China). Cell culture media components, including high glucose DMEM, α -MEM, fetal bovine serum (FBS), and antibiotics, were obtained from Gibco Chemicals (Grand Island, NY, USA). Cell counting kit-8 (CCK-8) was obtained from Dojindo Laboratories (Tokyo, Japan). The bicinchoninic acid (BCA) Protein Assay Kit for measuring protein concentrations was purchased from Pierce Biotechnology (Rockford, IL, USA). Polyvinylidene fluoride (PVDF) membranes were purchased from Millipore (Millipore, Billerica, MA, USA). Primary antibodies against LC3, P62, and glyceraldehyde 3-phosphate dehydrogenase (GAPDH) were obtained from Cell Signaling Technology (Beverly, MA, USA), and PINK1 and Parkin antibodies were obtained from Abcam (Cambridge, MA, USA). The Lipofectamine 2000 transfection reagent was obtained from Invitrogen (Carlsbad, CA, USA). Green fluorescent protein

(GFP)-LC3 was a kind gift from Professor Tanfeng, Wenzhou Medical University, Wenzhou, China.

NP characterization and suspension

The physical characteristics, original particle size, and surface morphologies of NPs were detected by transmission electron microscopy (TEM). Briefly, NPs were dispersed in ethanol and ultrasonicated for 10 min, and the suspension was then dropped onto a copper net. After the sample was dried, a conductive gold film was used to plate the surface of the sample using anion sputtering instrument. The samples were analyzed by TEM with an accelerating voltage of 200 kV. The dynamic light scattering method was used to determine the average hydrous particle size and zeta potential of the NPs. Briefly, NPs were suspended, ultrasonicated in deionized water, and analyzed using a Zetasizer Nano-ZS instrument (Malvern Instruments Ltd., Malvern, UK). Moreover, the X-ray diffraction (XRD) patterns of NPs were analyzed using an RAX-10X-ray diffractometer (Rigaku, Tokyo, Japan).

NP suspensions

ZnO NPs were dispersed and ultrasonicated in deionized water to obtain a uniformly dispersed NP suspension with a concentration of 10 mg/mL.

Cell culture and transfection

CAL 27 cells were cultured in DMEM containing 10% FBS and antibiotics at 37°C in a humidified chamber with a 5% CO₂-95% air mixture. Cells were seeded at a density of 5×10³, 2×10⁴, or 3×10⁵ cells/well in 96-well, 24-well, or 6-well plates, respectively, to meet the different needs of the experiments. On the next day, the cells were transfected with a Lipofectamine 2000 and GFP-LC3 plasmid mixture for 24 h. After transfection, the ZnO NP suspension was added to the culture media for further experiments.

Cytotoxicity assay

The cytotoxicity of ZnO NPs toward CAL 27 cells was evaluated using the CCK-8 assay. Briefly, the cells were cultured in 96-well plates at a density of 5×10³ cells/well and exposed to different concentrations (0, 5, 10, 20, 30, 40, 50, 60, 70, 80, 90, or 100 µg/mL) of ZnO NPs for 24 h. Cytotoxicity was expressed as a percentage of the control, and 50% inhibitory concentration (IC₅₀) values were calculated using GraphPad Prism software version 5.01.

Mitochondrial isolation and western blotting

Western blotting was used to detect the expression of target proteins. Briefly, CAL 27 cells cultured in 100-mm round

culture plates were treated with 25 µg/mL ZnO NPs at preset time points (4, 8, 12, or 24 h). Following treatment, cells were collected and lysed, and the mitochondrial as well as total and cytoplasmic proteins were extracted using the Cell Mitochondria Isolation Kit and radioimmunoprecipitation assay lysis buffer, respectively. Untreated cells served as the control. All protein extracts were electrophoresed on 10% (w/v) sodium dodecyl sulfate-polyacrylamide gels and then transferred to PVDF membranes. The membranes were then blocked with tris-buffered saline with Tween 20 containing 5% nonfat milk for 1 h at room temperature. After blocking, the membranes were incubated with the following primary antibodies (1:1,000) overnight at 4°C: GAPDH, LC3, P62, PINK1, and Parkin. The membranes were then washed and incubated with an IRDye800 fluorophore-conjugated secondary antibody for 1 h. Bands representing the antibody-antigen complexes were detected using an LI-COR Odyssey Infrared Imaging System.

Immunocytochemistry

CAL 27 cells treated with or without ZnO NPs were fixed with 4% paraformaldehyde for 15 min at 4°C. After fixation, the cells were incubated with primary antibodies (1:100) against LC3 and PINK1 overnight at 4°C. On the next day, the cells were washed gently with PBS 3 times and then incubated with a tetramethylrhodamine isothiocyanate-conjugated secondary antibody for 40 min at room temperature. Then, the cell nucleus was labeled with 4',6-diamidino-2-phenylindole for 10 min. The fluorescence of the antibody-antigen complex was detected by fluorescence microscopy or confocal laser scanning microscopy (CLSM).

Measurement of the intracellular ROS levels

The DCFH-DA probe was used to measure the intracellular ROS levels. Briefly, CAL 27 cells cultured in 96-well culture plates were treated with or without 25 µg/mL ZnO NPs for 4, 8, 12, or 24 h. After treatment, the cells were washed and labeled with the DCFH-DA probe (10 µM) for 1 h at 37°C. Subsequently, the average DCF fluorescence intensity in each well was detected using a Synergy-4 microplate reader (Biotek Instruments Inc., Winooski, VT, USA) (excitation 338 nm/emission 500 nm).

MDC staining

MDC staining was used to evaluate the number of autophagic vacuoles in CAL 27 cells. Briefly, CAL 27 cells cultured in 6-well culture plates were treated with or without 25 µg/mL ZnO NPs for 4, 8, 12, or 24 h. Following treatment, the cells

were collected and incubated with MDC for 30 min at 37°C. After staining, the average MDC fluorescence of each well was detected using a Synergy-4 microplate reader (excitation 338 nm/emission 500 nm).

JC-1 assay

A tetraethylbenzimidazolylcarbocyanine iodide (JC-1) dye was used to detect the MMP ($\Delta\Psi_m$) of CAL 27 cells. In healthy mitochondria, the JC-1 stain is present in an aggregated form and emits red fluorescence. However, in damaged or dysfunctional mitochondria, it remains in monomer form and emits green fluorescence. Briefly, CAL 27 cells cultured in 96-well culture plates were treated with or without 25 µg/mL ZnO NPs for 4, 8, 12, or 24 h. Then, the cells were collected and incubated with JC-1 for specified times. The samples were then immediately detected using the Synergy-4 microplate reader (excitation 540 nm/emission 590 nm to detect JC-1 aggregates and excitation 490 nm/emission 525 nm to detect JC-1 monomers).

Statistical analysis

The experimental data are presented as the means \pm SEM. At least 3 independent experiments were conducted to obtain objective and accurate data. SPSS software version 20 was used to analyze the data. Differences between groups were assessed using one-way analysis of variance. A detailed description of the statistical analysis used in each experiment is provided in the figure and table legends. Differences with *P*-values <0.05 were considered statistically significant. All western blot results were quantified using ImageJ 1.48v software.

Results

Characterization of NPs

The original sizes and surface morphologies of ZnO NPs were detected using TEM. The original shape of these particles was a hexagonal prism, and the original size was ~50 nm (Figure 1A). The results of the XRD spectra showed that the peaks of the pending particles were consistent with ZnO standards, according to the Committee on Powder Diffraction Standards (JCPDS 36-1451) (Figure 1B). The average hydrous size of NPs in deionized water was ~500.8 nm, indicating that aggregates of ZnO NPs formed in a deionized water solution (Figure 1C).

Effect of ZnO NPs on CAL 27 cell viability

ZnO NPs increased the intracellular ROS levels and induced cell death or apoptosis in CAL 27 cells. We first investigated

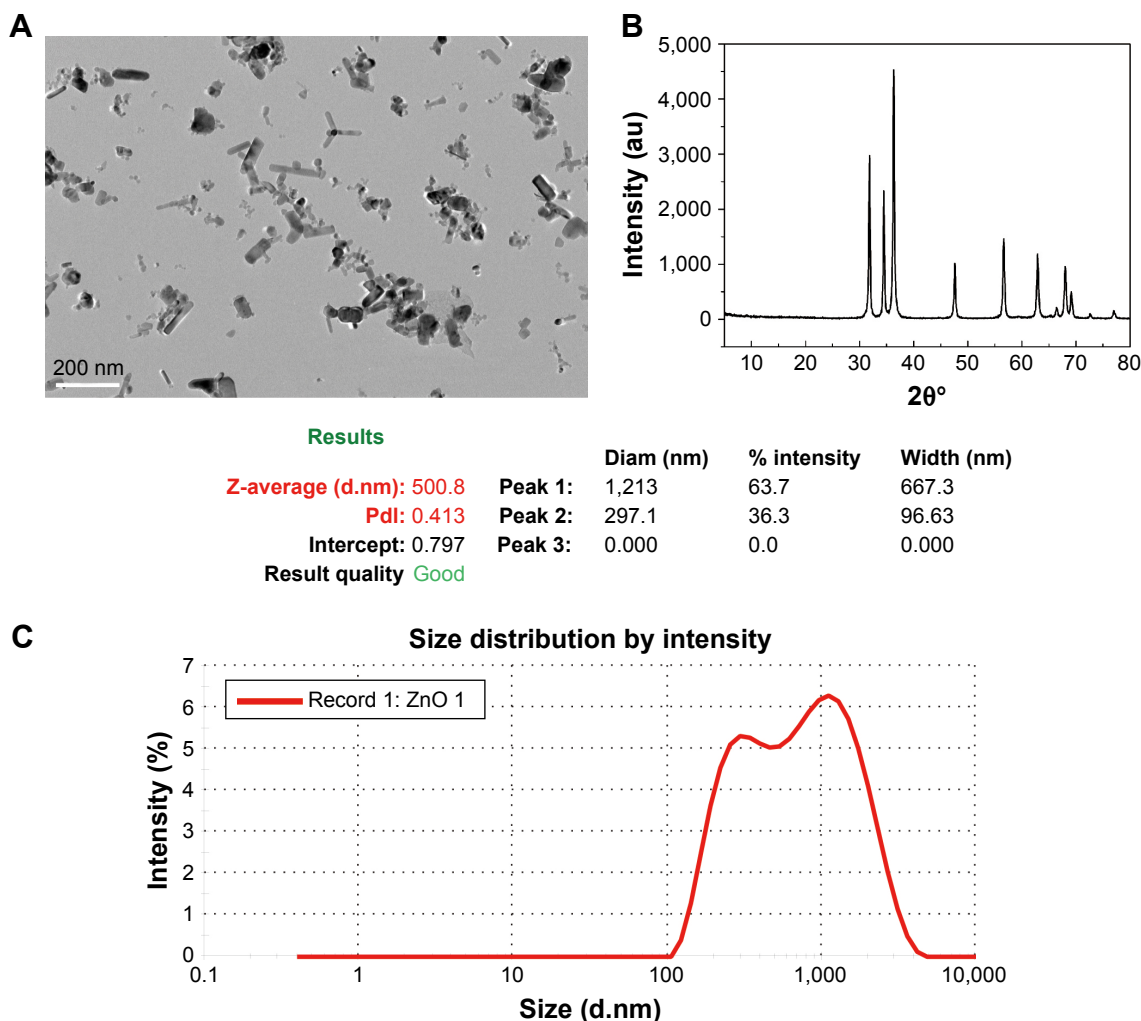


Figure 1 Characterization of ZnO NPs.

Notes: (A) TEM image indicating that the original shape of particles was a hexagonal prism and the original size was ~50 nm. (B) X-ray diffraction pattern of ZnO NPs. (C) Average hydrous size of ZnO NPs in deionized water.

Abbreviations: Diam, diameter; Pdl, polydispersity index; TEM, transmission electron microscopy; ZnO NPs, zinc oxide nanoparticles.

the effects of ZnO NPs on the viability of CAL 27 cells using the CCK-8 assay. After treatment with different concentrations of ZnO NPs for 24 h, the viability of CAL 27 cells decreased following treatment with increasing ZnO NP concentrations (Figure 2A). The IC₅₀ of the ZnO NPs was calculated as 25 µg/mL.

ZnO NPs induced mitochondrial damage and oxidative stress in CAL 27 cells

The oxidative status of CAL 27 cells treated with 25 µg/mL ZnO NPs was determined using the DCFH-DA probe. Compared with the control, significantly higher ROS levels were detected 4, 8, and 12 h after ZnO NP treatment (Figure 2B), suggesting that mitochondrial oxidative damage may contribute to ZnO NP-induced cell apoptosis. The MMP was evaluated using the JC-1 assay, and the results revealed a

decrease in the MMP of cells treated with 25 µg/mL ZnO NPs for 4, 8, 12, or 24 h, suggesting the onset of mitochondrial dysfunction (Figures 2C and 3A). Furthermore, the TEM images showed an increased number of swollen mitochondria in the 12-h group (Figure 3B). Thus, exposure to 50 nm ZnO NPs induced mitochondrial dysfunction in CAL 27 cells.

ZnO NPs triggered the autophagy process in CAL 27 cells

Autophagic vacuoles were first measured using the MDC assay, and the result revealed an increase in the MDC fluorescence intensity in the groups that had been treated with ZnO NPs for 4, 8, 12, or 24 h (Figure 2D), indicating that ZnO NPs induced the autophagy process shortly after administration. We investigated the expression of the autophagy-related proteins LC3, P62, and Beclin1 by immunocytochemistry and

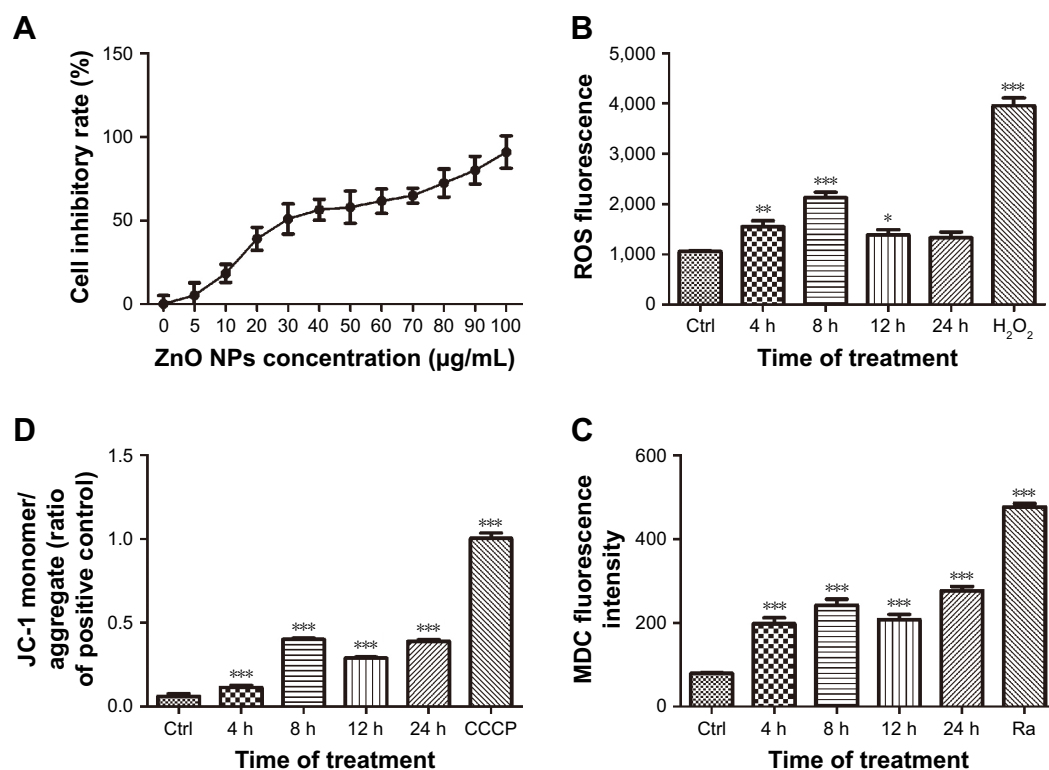


Figure 2 (A) Effects of various concentrations of ZnO NPs on the cell inhibitory rate of CAL 27 cells. Cells were cultured in 96-well plates and treated with 0, 5, 10, 20, 30, 40, 50, 60, 70, 80, 90, or 100 µg/mL ZnO NPs for 24 h. According to the results of the CCK-8 assay, 25 µg/mL ZnO NPs decreased the cell viability to <50% ($P < 0.001$). **(B–D)** After treatment with or without 25 µg/mL ZnO NPs for 4, 8, 12, or 24 h, the cells were incubated with the DCFH-DA probe, JC-1 or MDC, and then measured using a Synergy-4 microplate reader. Cells treated with H₂O₂ (500 mM) for 2 h, CCCP (10 µM) for 20 min, and rapamycin (100 nM) for 2 h served as positive controls in each of the aforementioned experiments, respectively. The data are presented as the mean ± SEM ($n = 6$). * $P < 0.05$; ** $P < 0.01$; *** $P < 0.001$.

Abbreviations: Ctrl, control; CCK-8, cell counting kit-8; DCFH-DA, 2',7'-dichlorofluorescein diacetate; JC-1, tetraethylbenzimidazolylcarbocyanine iodide; MDC, monodansylcadaverine; ROS, reactive oxygen species; SEM, standard error of measurement; ZnO NPs, zinc oxide nanoparticles; Ra, rapamycin.

western blotting to further examine the molecular mechanism through which ZnO NPs induced autophagy. As shown in Figure 4A–C, ZnO NPs significantly increased the expression of LC3II and Beclin 1 and decreased the expression of P62 in a time-dependent manner. Then, CAL 27 cells were transfected with a GFP-LC3 plasmid and treated with ZnO NPs, an increasing number of GFP-LC3 puncta was observed in the experimental groups, indicating an increase in the number of autolysosomes (Figure 5A). Furthermore, the TEM micrographs showed an increasing number of autolysosomes in the 8-h group, as shown in Figure 4D. Based on these findings, ZnO NPs induced autophagy in CAL 27 cells.

ZnO NPs induced PINK1/Parkin-mediated mitophagy in CAL 27 cells

In the classical mitophagy process, Parkin is selectively recruited from the cytoplasm to the outer membrane of the damaged mitochondrion through the accumulation of PINK1, which ultimately promotes the degradation of dysfunctional mitochondria.^{20,21} In the present study, the expression of the total Parkin, mito-Parkin, cyto-Parkin,

and PINK1 proteins was evaluated by western blotting. Elevated Parkin levels were observed in the mitochondria and decreased Parkin expression was observed in the cytoplasm following treatment with ZnO NPs (Figure 5A), indicating that Parkin translocated from the cytoplasm to the mitochondria during the stimulation period. Moreover, increased PINK1 expression was observed after the ZnO NP treatment, indicating that the decreased MMP in damaged mitochondria stabilized PINK1 in the outer mitochondrial membrane (Figure 5A). CAL 27 cells were first transfected with the GFP-LC3 plasmid before treatment to further investigate the molecular mechanism through which PINK1 affected ZnO NP-induced cytotoxicity. PINK1 expression was evaluated by immunocytochemistry using CLSM. As shown in Figure 5B, increasing numbers of green GFP-LC3 puncta and red PINK1 puncta were observed, and greater co-localization of LC3 and PINK1 puncta was observed in the experimental groups, indicating the accumulation of mitolysosomes. Therefore, the balance between mitochondrial accumulation and degradation was destroyed in CAL 27 cells after ZnO NP treatment.

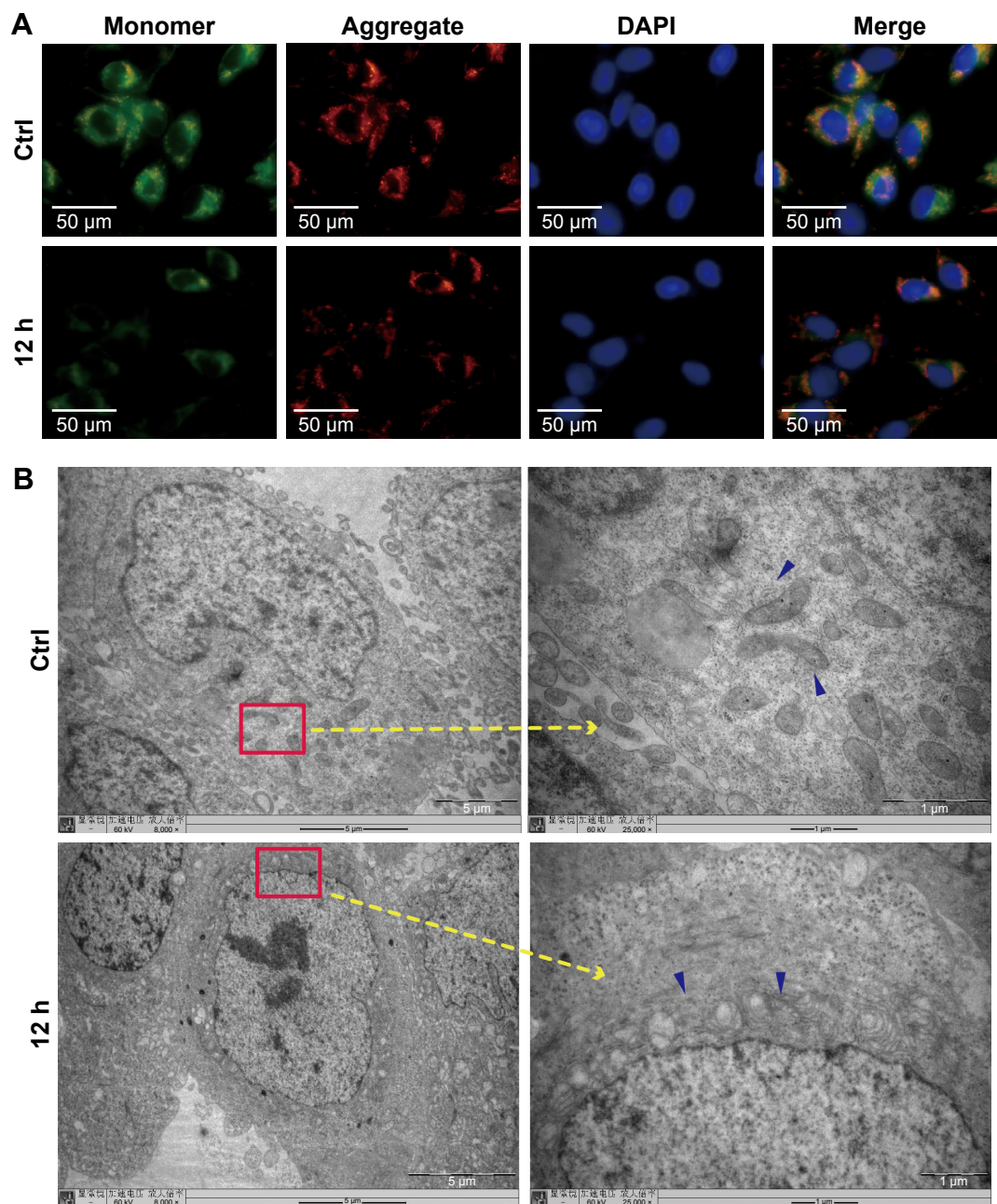


Figure 3 Effect of ZnO NPs on the MMP in CAL 27 cells.

Notes: Cells were treated with or without 25 $\mu\text{g}/\text{mL}$ ZnO NPs for 12 h. **(A)** The cells were then incubated with JC-1 for specified times, and the fluorescence intensity was evaluated using fluorescence microscopy. **(B)** Alterations in the shape of the mitochondria were detected by TEM. Blue arrows show the mitochondria, and the images revealed a greater number of swollen mitochondria around the nucleus in the experimental groups than in the control.

Abbreviations: Ctrl, control; JC-1, tetraethylbenzimidazolylcarbocyanine iodide; MMP, mitochondrial membrane potential; TEM, transmission electron microscopy; ZnO NPs, zinc oxide nanoparticles.

Discussion

ZnO is a multi-functional metal oxide. Because of the excellent performance of ZnO NPs as an antibacterial agent, disinfectant, and UV shield, among others, they have been widely used in antibacterial and anti-ultraviolet products, as well as in other medical fields.^{22,23} More recently, the important role of ZnO NPs in tumor therapy has attracted extensive attention. ZnO NPs show a strong anticancer effect on some

cancer cell types; for example, ZnO NPs selectively induce cell death in human HNSCC *in vitro*.¹¹ ZnO NPs have been shown to increase the death of both human malignant melanoma A375 and mouse skin melanoma B16F10 cell lines, and these NPs also inhibit tumor growth in a BALB/C-B16F10 mouse melanoma model.²⁴

We first evaluated CAL 27 cell viability following treatment with various ZnO NP concentrations to determine

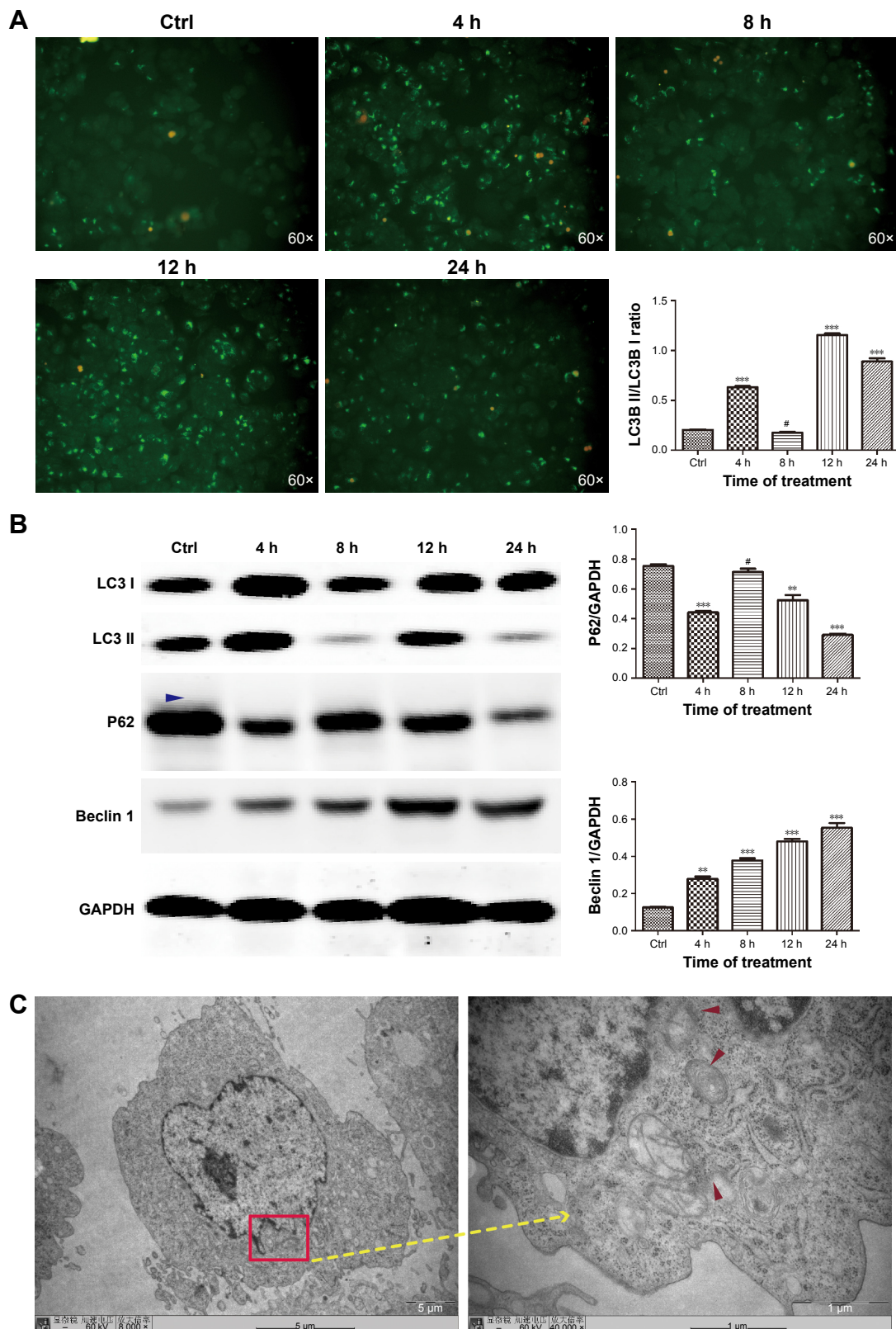


Figure 4 ZnO NPs induced autophagy in CAL 27 cells.

Notes: (A) After treatment with or without 25 μ g/mL ZnO NPs for 4, 8, 12, or 24 h, cells were fixed with 4% paraformaldehyde and incubated with diluted LC3 primary antibodies (1:100) overnight at 4°C. On the next day, the cells were incubated with a tetramethylrhodamine isothiocyanate-conjugated secondary antibody for 40 min at 37°C. LC3 staining was visualized using fluorescence microscopy. (B) Cells were harvested and lysed, and the expression of LC3, P62, and Beclin I was then detected by Western blotting. (C) The autophagosomes in the experimental groups were detected by TEM. Red arrows show autophagosomes, and the images showed an increasing number of autophagosomes in the experimental groups. # P >0.05; ** P <0.01; *** P <0.001.

Abbreviations: Ctrl, control; TEM, transmission electron microscopy; ZnO NPs, zinc oxide nanoparticles.

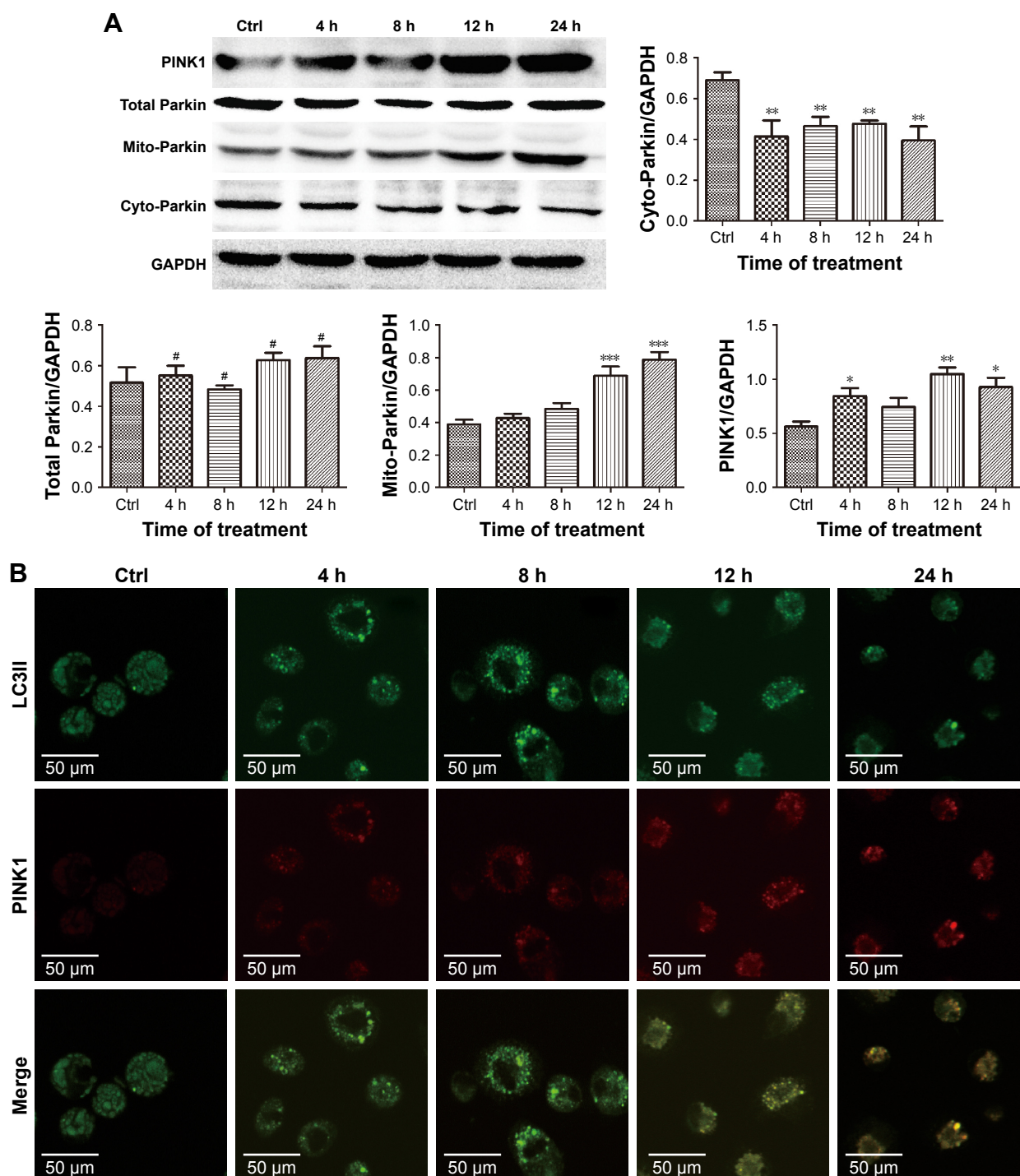


Figure 5 ZnO NPs activated PINK1/Parkin-mediated mitophagy in CAL 27 cells.

Notes: After transfection with the GFP-LC3 plasmid, the cells were treated with or without 25 $\mu\text{g/mL}$ ZnO NPs for 4, 8, 12, or 24 h. **(A)** The cells were then harvested and lysed, and the levels of the total Parkin, mito-Parkin, and cyto-Parkin proteins were evaluated by Western blotting. **(B)** Cells were harvested and then stained with IF-IC using the PINK1 antibody, and the expression of PINK1 and LC3 was determined using CLSM. $^{\#}P > 0.05$; $^*P < 0.05$; $^{**}P < 0.01$; $^{***}P < 0.001$.

Abbreviations: Ctrl, control; CLSM, confocal laser scanning microscopy; ZnO NPs, zinc oxide nanoparticles.

whether ZnO NPs are cytotoxic toward CAL 27 cells. The results of our present study revealed the anticancer activity of ZnO NPs toward CAL 27 cells. ZnO NPs induced cell death or apoptosis in both dose- and time-dependent manner. These results are consistent with findings from previous

studies.^{10,25} ZnO NP-induced cytotoxicity in cancer cells is associated with ROS production. Chakraborti et al claimed that PEG-modified ZnO NPs display anticancer properties mainly due to the formation of ROS.²⁶ In the mechanistic study by Wang et al, ZnO NP treatments induced apoptosis

in LTEPa-2 human pulmonary adenocarcinoma cells by increasing the intracellular ROS levels.²⁷ Kim et al observed that exposure of A549 cells to ZnO NPs in vitro was associated with reduced levels of oxidative stress biomarkers.²⁸ In many previous studies, the mitochondrial electron transport chain was considered the main source of cellular ROS. We evaluated alterations of the MMP, the intracellular ROS levels, and the shape of the mitochondria following ZnO NP treatment. ZnO NPs increased the intracellular ROS level and decreased the MMP in CAL 27 cells. Moreover, the TEM micrographs suggested an increase in nonfunctional swelling of the mitochondria after ZnO NP treatment, implying that ZnO NPs may induce cell death by generating mitochondrial damage and ROS.

According to Johnson et al, ZnO NPs induce immune cell death by increasing ROS generation and inhibiting the autophagy process.²⁹ However, Hackenberg et al found that the combination of a photocatalytic treatment with both ZnO NPs and UVA-1 significantly increased the levels of LC3 II and ROS in HNSCC.³⁰ In the study by Yu et al, an increased accumulation of abnormal autophagic vacuoles and damaged mitochondria was detected in normal skin cells treated with ZnO NPs. Moreover, decreases in the MMP and ATP production were observed after co-culture with ZnO NPs. The induction of autophagy via ROS production is postulated to be the main cause of cell death.³¹ In conclusion, nanoscale ZnO may stimulate or inhibit autophagy to promote cell death, depending on the cell type. In the present study, increased levels of LC3II were detected in cells treated with ZnO NPs, indicating induction of the autophagy process.

Mitophagy, a special autophagic process, involves the selective clearance of dysfunctional mitochondria labeled by the autophagy-related receptor system in cells. Mitochondria are key organelles required for cellular energy metabolism and regulate signal transduction and apoptosis in mammalian cells. Mitophagy maintain the number and quality of mitochondria in the cells by periodically scavenging damaged, aging or redundant mitochondria through a variety of complex mechanisms. The PINK1/Parkin pathway is accepted as one of the major molecular mechanisms regulating the mitophagy process. PINK1 is a protein kinase that is mainly located in the outer mitochondrial membrane.³² Parkin is an E3 ubiquitin ligase 8 located in the cytoplasm. In damaged mitochondria, Parkin is phosphorylated by PINK1 at S65, inducing the translocation of Parkin from the cytoplasm to the mitochondria and subsequently enabling Parkin-mediated ubiquitination of other proteins.³³ We examined whether ZnO NPs induce the expression of mitophagy-related proteins to confirm that the PINK1/Parkin-mediated mitophagy process

participates in ZnO NP-induced cytotoxicity. As expected, increased levels of LC3-II, PINK1, and mito-Parkin and decreased levels of P62 and cyto-Parkin were observed following treatment with 25 $\mu\text{g}/\text{mL}$ ZnO NPs. Notably, this effect was observed in a time-dependent manner. Based on these results, ZnO NPs activated the PINK1/Parkin-mediated mitophagy process in CAL 27 cells.

Mitophagy has been reported to play dual roles in cancer cells:³⁴ it facilitates cell survival by allowing adaptations to stress or promotes cell death through the excessive removal of mitochondria.³⁵ Sentelle et al showed that mitophagy induction promotes tumor cell death via a mechanism involving autophagy.³⁶ To investigate the specific role of PINK1/Parkin-mediated mitophagy in ZnO NP-induced toxicity, we transfected cells with GFP-LC3 to locate the autophagosomes and used the red fluorescent PINK1 puncta to identify the damaged mitochondria. The results revealed increased co-localization of green and red puncta following ZnO NP treatment, indicating that ZnO NPs induced cytotoxicity in CAL 27 cells through excessive formation of mitolysosomes.

Conclusion

The ZnO NP-induced cytotoxicity toward CAL 27 cells may be at least partially mediated by the induction of PINK1/Parkin-mediated mitophagy. This study is the first to show a link between ZnO NP-induced mitophagy and cytotoxicity in CAL 27 cells. Therefore, ZnO NPs may possess potential anticancer activity toward tongue cancer cells. These in vitro results are very encouraging, and further in vivo studies are being conducted. We believe that this work offers a promising foundation for the clinical application of ZnO NPs as a treatment for tongue cancer and could lead to the development of new strategies for tongue cancer treatment.

Acknowledgments

This work was supported by grants from the Zhejiang Provincial Natural Science Foundation of China (LY16H140003 and LY17H140008) and the Wenzhou Municipal Science and Technology Bureau Foundation of China (Y20150070 and Y20150256).

Author contributions

LW conceived and designed the experiments. JW, ZX, and SW performed the experiments. JW analyzed the data and contributed reagents, materials and analytical tools. LW wrote the paper. All authors contributed to the data analysis, drafting of the manuscript, and critical revisions of the paper, and they agree to be accountable for all aspects of the work.

Disclosure

The authors report no conflicts of interest in this work.

References

- Sagheb K, Kumar V, Rahimi-Nedjat R, et al. Cervical metastases behavior of T1-2 squamous cell carcinoma of the tongue. *J Maxillofac Oral Surg*. 2017;16(3):300–305.
- Zhang YY, Wang DC, Su JZ, Jia LF, Peng X, Yu GY. Clinicopathological characteristics and outcomes of squamous cell carcinoma of the tongue in different age groups. *Head Neck*. 2017;39(11):2276–2282.
- Safi AF, Grandoch A, Nickenig HJ, Zoller JE, Kreppel M. The importance of lymph node ratio for locoregional recurrence of squamous cell carcinoma of the tongue. *J Craniomaxillofac Surg*. 2017;45(7):1058–1061.
- Abdalla AME, Xiao L, Ullah MW, Yu M, Ouyang C, Yang G. Current challenges of cancer anti-angiogenic therapy and the promise of nanotherapeutics. *Theranostics*. 2018;8(2):533–548.
- Bhise K, Sau S, Alsaab H, Kashaw SK, Tekade RK, Iyer AK. Nanomedicine for cancer diagnosis and therapy: advancement, success and structure-activity relationship. *Ther Deliv*. 2017;8(11):1003–1018.
- Guimaraes PPG, Gaglione S, Sewastianik T, Carrasco RD, Langer R, Mitchell MJ. Nanoparticles for immune cytokine TRAIL-based cancer therapy. *ACS Nano*. 2018;12(2):912–931.
- Memarzadeh K, Sharili AS, Huang J, Rawlinson SC, Allaker RP. Nanoparticulate zinc oxide as a coating material for orthopedic and dental implants. *J Biomed Mater Res A*. 2015;103(3):981–989.
- Javid M, Zarei M, Naghavi N, Mortazavi M, Nejat AH. Zinc oxide nano-particles as sealer in endodontics and its sealing ability. *Contemp Clin Dent*. 2014;5(1):20–24.
- Osmond MJ, McCall MJ. Zinc oxide nanoparticles in modern sunscreens: an analysis of potential exposure and hazard. *Nanotoxicology*. 2010;4(1):15–41.
- Hassan HF, Mansour AM, Abo-Youssef AM, Elsadek BE, Messiha BA. Zinc oxide nanoparticles as a novel anticancer approach; in vitro and in vivo evidence. *Clin Exp Pharmacol Physiol*. 2017;44(2):235–243.
- Gehrke T, Scherzad A, Ickrath P, et al. Zinc oxide nanoparticles antagonize the effect of Cetuximab on head and neck squamous cell carcinoma in vitro. *Cancer Biol Ther*. 2017;18(7):513–518.
- Yin H, Casey PS, McCall MJ, Fenech M. Size-dependent cytotoxicity and genotoxicity of ZnO particles to human lymphoblastoid (WIL2-NS) cells. *Environ Mol Mutagen*. 2015;56(9):767–776.
- Wang J, Lee JS, Kim D, Zhu L. Exploration of Zinc Oxide Nanoparticles as a Multitarget and Multifunctional Anticancer Nanomedicine. *ACS Appl Mater Interfaces*. 2017;9(46):39971–39984.
- van der Blik AM, Sedensky MM, Morgan PG. Cell Biology of the Mitochondrion. *Genetics*. 2017;207(3):843–871.
- Qian H, Chao X, Ding WX. A PINK1-mediated mitophagy pathway decides the fate of tumors-to be benign or malignant? *Autophagy*. 2018;14(4):563–566.
- Yang C, Suda T. Hyperactivated mitophagy in hematopoietic stem cells. *Nat Immunol*. 2018;19(1):2–3.
- Yan C, Li TS. Dual role of mitophagy in cancer drug resistance. *Anticancer Res*. 2018;38(2):617–621.
- Bai DP, Zhang XF, Zhang GL, Huang YF, Gurunathan S. Zinc oxide nanoparticles induce apoptosis and autophagy in human ovarian cancer cells. *Int J Nanomedicine*. 2017;12:6521–6535.
- Wang B, Zhang J, Chen C, et al. The size of zinc oxide nanoparticles controls its toxicity through impairing autophagic flux in A549 lung epithelial cells. *Toxicol Lett*. 2018;285:51–59.
- Zhang Z, Zhou L, Zhou Y, et al. Mitophagy induced by nanoparticle-peptide conjugates enabling an alternative intracellular trafficking route. *Biomaterials*. 2015;65:56–65.
- Pickrell AM, Youle RJ. The roles of PINK1, parkin, and mitochondrial fidelity in Parkinson's disease. *Neuron*. 2015;85(2):257–273.
- Suarez DF, Monteiro APF, Ferreira DC, et al. Efficient antibacterial nanosponges based on ZnO nanoparticles and doxycycline. *J Photochem Photobiol B*. 2017;177:85–94.
- Laurenti M, Cauda V. ZnO Nanostructures for tissue engineering applications. *Nanomaterials (Basel)*. 2017;7(11):374.
- Ramani M, Mudge MC, Morris RT, et al. Zinc oxide nanoparticle-poly I:C RNA complexes: implication as therapeutics against experimental melanoma. *Mol Pharm*. 2017;14(3):614–625.
- Moratin H, Scherzad A, Gehrke T, et al. Toxicological characterization of ZnO nanoparticles in malignant and non-malignant cells. *Environ Mol Mutagen*. 2018;59(3):247–259.
- Chakraborti S, Chakraborty S, Saha S, et al. PEG-functionalized zinc oxide nanoparticles induce apoptosis in breast cancer cells through reactive oxygen species-dependent impairment of DNA damage repair enzyme NEIL2. *Free Radic Biol Med*. 2017;103:35–47.
- Wang C, Hu X, Gao Y, Ji Y. ZnO Nanoparticles treatment induces apoptosis by increasing intracellular ROS levels in LTP-a-2 cells. *Biomed Res Int*. 2015;2015:423287.
- Kim E, Jeon WB, Kim S, Lee SK. Decrease of reactive oxygen species-related biomarkers in the tissue-mimic 3D spheroid culture of human lung cells exposed to zinc oxide nanoparticles. *J Nanosci Nanotechnol*. 2014;14(5):3356–3365.
- Johnson BM, Fraietta JA, Gracias DT, et al. Acute exposure to ZnO nanoparticles induces autophagic immune cell death. *Nanotoxicology*. 2015;9(6):737–748.
- Hackenberg S, Scherzad A, Gohla A, et al. Nanoparticle-induced photocatalytic head and neck squamous cell carcinoma cell death is associated with autophagy. *Nanomedicine (Lond)*. 2014;9(1):21–33.
- Yu KN, Yoon TJ, Minai-Tehrani A, et al. Zinc oxide nanoparticle induced autophagic cell death and mitochondrial damage via reactive oxygen species generation. *Toxicol In Vitro*. 2013;27(4):1187–1195.
- Trempe JF, Sauve V, Grenier K, et al. Structure of parkin reveals mechanisms for ubiquitin ligase activation. *Science*. 2013;340(6139):1451–1455.
- Manzanillo PS, Ayres JS, Watson RO, et al. The ubiquitin ligase parkin mediates resistance to intracellular pathogens. *Nature*. 2013;501(7468):512–516.
- Wang K, Klionsky DJ. Mitochondria removal by autophagy. *Autophagy*. 2011;7(3):297–300.
- Kulik AV, Luchkina EA, Gogvadze V, Zhivotovsky B. Mitophagy: link to cancer development and therapy. *Biochem Biophys Res Commun*. 2017;482(3):432–439.
- Sentelle RD, Senkal CE, Jiang W, et al. Ceramide targets autophagosomes to mitochondria and induces lethal mitophagy. *Nat Chem Biol*. 2012;8(10):831–838.

International Journal of Nanomedicine

Publish your work in this journal

The International Journal of Nanomedicine is an international, peer-reviewed journal focusing on the application of nanotechnology in diagnostics, therapeutics, and drug delivery systems throughout the biomedical field. This journal is indexed on PubMed Central, MedLine, CAS, SciSearch®, Current Contents®/Clinical Medicine,

Submit your manuscript here: <http://www.dovepress.com/international-journal-of-nanomedicine-journal>

Dovepress

Journal Citation Reports/Science Edition, EMBASE, Scopus and the Elsevier Bibliographic databases. The manuscript management system is completely online and includes a very quick and fair peer-review system, which is all easy to use. Visit <http://www.dovepress.com/testimonials.php> to read real quotes from published authors.